Simulating crop yield losses in Switzerland for historical and present Tambora climate scenarios

2017 Environ. Res. Lett. 12 074026

(http://iopscience.iop.org/1748-9326/12/7/074026)

Environmental Research Letters

LETTER

Simulating crop yield losses in Switzerland for historical and present Tambora climate scenarios

Simon Flückiger[1,2], Stefan Brönnimann[1,2,5], Annelie Holzkämper[2,3], Jürg Fuhrer[2,3], Daniel Krämer[2,4], Christian Pfister[2,4] and Christian Rohr[2,4]

[1] Institute of Geography, University of Bern, Bern, Switzerland
[2] Oeschger Centre for Climate Change Research, University of Bern, Bern, Switzerland
[3] Agroscope, Zurich, Switzerland
[4] Institute of History, University of Bern, Bern, Switzerland
[5] Author to whom any correspondence should be addressed.

E-mail: stefan.broennimann@giub.unibe.ch

Keywords: Tambora, weather reconstruction, crop model, year without a summer

Supplementary material for this article is available online

OPEN ACCESS

RECEIVED
17 February 2017

REVISED
25 April 2017

ACCEPTED FOR PUBLICATION
10 May 2017

PUBLISHED
19 July 2017

Abstract

Severe climatic anomalies in summer 1816, partly due to the eruption of Tambora in April 1815, contributed to delayed growth and poor harvests of important crops in Central Europe. Coinciding with adverse socio-economic conditions, this event triggered the last subsistence crisis in the western World. Here, we model reductions in potential crop yields for 1816 and 1817 and address the question, what impact a similar climatic anomaly would have today. We reconstructed daily weather for Switzerland for 1816/17 on a 2 km grid using historical observations and an analogue resampling method. These data were used to simulate potential crop yields for potato, grain maize, and winter barley using the CropSyst model calibrated for current crop cultivars. We also simulated yields for the same weather anomalies, but referenced to a present-day baseline temperature. Results show that reduced temperature delayed growth and harvest considerably, and in combination with reduced solar irradiance led to a substantial reduction (20%–50%) in the potential yield of potato in 1816. Effects on winter barley were smaller. Significant reductions were also modelled for 1817 and were mainly due to a cold late spring. Relative reductions for the present-day scenario for the two crops were almost indistinguishable from the historical ones. An even stronger response was found for maize, which was not yet common in 1816/17. Waterlogging, which we assessed using a stress-day approach, likely added to the simulated reductions. The documented, strong east-west gradient in malnutrition across Switzerland in 1817/18 could not be explained by biophysical yield limitations (though excess-water limitation might have contributed), but rather by economic, political and social factors. This highlights the importance of these factors for a societies' ability to cope with extreme climate events. While the adaptive capacity of today's society in Switzerland is much greater than in the early 19th century, our results emphasize the need for interdisciplinary approaches to climate change adaptation considering not only biophysical, but also social, economic and political aspects.

1. Introduction

The eruption of Tambora in April 1815 affected global weather and climate (Oppenheimer 2003, Luterbacher and Pfister 2015, Raible *et al* 2016, Brönnimann and Krämer 2016). Partly due to the volcanic eruption (but also due to large random variability), the summer of 1816 was very cold and wet in Central Europe, and 1816 became known as a 'Year Without a Summer' (YWAS). Average temperatures were 2 °C–3 °C below that of the preceding two decades, and the frequency of rainy days was strongly increased, although the climatic anomalies did not affect all parts of Europe equally (Veale and Endfield 2016, Brázdil *et al* 2016,

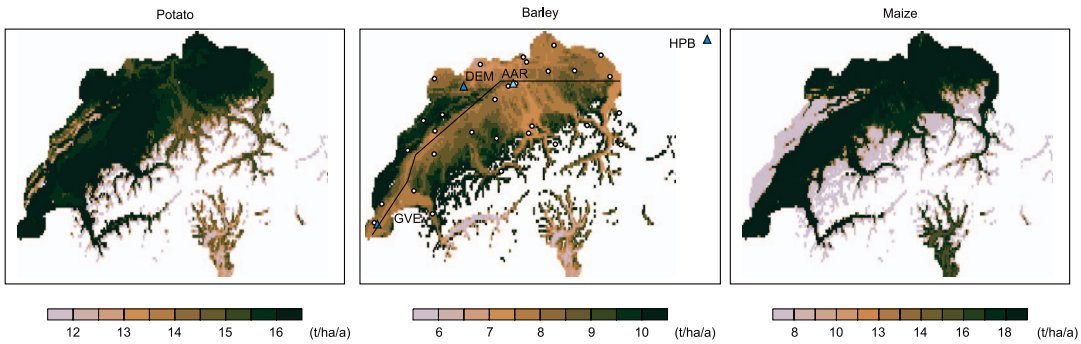

Figure 1. Potential crop yield (harvested biomass) in the present reference period for potato, winter barley, and maize, respectively. The middle panel shows the location of the meteorological stations used for the present period (circles) and for the historical period (triangles—the light blue triangle was used only for validation), HPB = Hohenpeissenberg) as well as the transect used. Only areas below 1500 m asl were calculated.

Luterbacher and Pfister 2015). In the most impacted regions, adverse weather conditions in 1816 delayed crop harvests and caused very poor yields (Krämer 2015). The crop yield losses were an additional factor on top of many others—empty storages after the coalition wars, economic downturn in proto-industrialized regions, new political responsibilities, etc.—that made societies in Central Europe vulnerable to crisis. In many places, increasing prices contributed to the last great subsistence crisis in Central Europe (Post 1977), to malnutrition, migration, low fertility, or death (Krämer 2015).

The YWAS of 1816 has been used as a test case for studying the resilience of the global food system to extreme climatic disturbances. Puma *et al* (2015) found that today a similar event could disrupt international trade networks due to crop losses in major production regions. The YWAS of 1816 can thus be considered as a 'worst case' scenario for the effects of strong climate variability on an inter-annual scale on regional crop yields and food security.

The aim of the present study is to investigate today's potential effects of such an extreme climatic event on crop yields with a focus on as a region that was most severely affected. Because both the weather situation in 1816 and the resulting crisis in 1816, and particularly in 1817, are historically well documented (Krämer 2015), the YWAS of 1816 is thus a suitable scenario to assess current crop sensitivities using a numerical modelling approach. Such an approach also allows to better separate the weather-related contribution to the crisis in 1817 from other influences. For instance, maps of malnutrition in 1817 and 1818 for Switzerland (Krämer 2015) show a pronounced east-west gradient across Switzerland, with the eastern region being more severely affected than the west, which may reflect differences in social, economic and political conditions (Krämer 2015), while the influence of small-scale differences in climatic conditions remains unclear.

Our numerical approach starts from historical instrumental weather data. We use a novel analogue resampling technique to reconstruct high-resolution daily weather data for 1815–1817 as well as for a corresponding scenario in today's warmer climate. The data are used to drive a crop model that simulates phenology and crop yield for selected crops. Some important factors such as soil wetness or the susceptibility to pests and diseases are not part of the crop model, but possible effects of water logging are assessed ex-post using an empirical approach. Also, historical information on the pattern of land use in 1816 is not available at the required level of detail, and thus only a measure of potentially attainable yield is calculated. Note also that only crop yield quantity and not quality could be simulated.

2. Data and methods

2.1. Weather data

The study made use of sub-daily historical meteorological information from four different stations from 1800–1820 The series of Geneva (Schüepp 1961, Auchmann *et al* 2012) and Hohenpeissenberg (Winkler 2009) are described in the literature (see figure 1). Each has twice daily data for temperature, pressure, and wind direction (among other variables), as well as daily precipitation sums. The series from Basel/Delémont (Bider *et al* 1959) is composed of several series and, for 1816/17, has only daily mean temperature and pressure. For the same series, we also used present-day data from automated weather stations in Switzerland reaching back to around 1980. These data included solar radiation.

In addition, and only for validation, we used a series from Aarau for 1816, which we discovered during writing the paper (Brugnara *et al* 2015). The series provides temperature together with qualitative information on precipitation observed by Heinrich Zschokke, published in the 'Archiv der Medicin, Chirurgie und Pharmacie' (digital.ub.uni-duesseldorf.de/ihd/periodical/pageview/7592104). A full description of the entire series follows elsewhere. Since we used the data only for one year and only in the form of correlations, the data could be used in raw form.

Table 1. Stations, altitude above sea level (asl), Swiss coordinates, and variables used (I = solar irradiance, P = pressure, RR = rain fall). Asterisks denote historical series.

Station	Abb	Altitude (m asl)	Swiss Coordinates	Variables
Aadorf/Tänikon	TAE	539	710515/259821	I, P
Aarau*	AAR	380	645737/249126	T, P
Aigle	AIG	381	560401/130713	I
Altdorf	ALT	438	690174/193558	I, P
Basel/Binnningen	BAS	316	610911/265601	I, P
Bern/Zollikofen	BER	552	601930/204410	I, P
Beznau	BEZ	325	659808/267694	I
Buchs/Aarau	BUS	386	648389/248365	I, P, T
Bullet/La Frétaz	FRE	1205	534221/188081	I
Chasseral	CHA	1599	570847/220158	I, P
Chur	CHU	556	759466/193153	I
Delémont/Delsberg*	DEM	439	593269/244543	I, T, wind
Fahy	FAH	596	562458/252676	I, P
Genéve-Cointrin*	GVE	420	498905/122632	I, P, T, RR, wind
Glarus	GLA	516	723752/210568	I, P
Gösgen	GOE	380	640417/245937	I
Güttingen	GUT	440	738420/273960	I, P
Hohenpeissenberg*	HPB	977		P, wind
Interlaken	INT	577	633019/169093	I, P
La Chaux-de-Fonds	CDF	1018	550919/214861	I, P
Langnau i.e.	LAG	745	628005/198792	I
Leibstadt	LEI	341	656379/272111	I
Luzern	LUZ	454	665540/209848	I
Neuchâtel	NEU	485	563087/205560	I, P
Nyon/Changins	CGI	455	506880/139573	I
Payerne	PAY	490	562127/184612	I, P
Pilatus	PIL	2106	661910/203410	I
Pully	PUY	455	540811/151514	I, P
Schaffhausen	SHA	438	688698/282796	I, P
St Gallen	STG	775	747865/254588	I
Vaduz	VAD	457	757719/221697	I, P
Wynau	WYN	422	626400/233850	I, P
Zürich/Kloten	KLO	426	682710/259339	I, P

As a reference we used gridded daily data for Switzerland (MeteoSwiss 2013a, 2013b, Frei 2013), encompassing daily minimum (T_{min}) and maximum (T_{max}) temperature as well as precipitation on a 2 km grid from 1961 to present. For solar radiation, we performed a weighted interpolation applying a *k*-nearest neighbour algorithm. We chose the nearest three stations from the Swiss meteorological network (figure 1, table 1) according to Euclidian distance.

2.2. Weather reconstruction approach

The crop model requires daily fields of T_{min} and T_{max}, precipitation and solar radiation at a high spatial resolution. In order to reconstruct these fields 1816, we used an analogue resampling approach of the 2 km gridded data. A schematic of the reconstruction is given in figure S1 available at stacks.iop.org/ERL/12/074026/mmedia. For each day, we sampled the daily fields from a present period according to their similarity with historical instrumental measurements, restricting the search to days of the same weather type and of the same season. This procedure ensured physical consistency of the derived reconstruction, although it required a sufficiently long training period (i.e. sufficiently large pool of analogues). The period was set to 1982–2009, for which not only temperature and precipitation, but also solar radiation data were available. The procedure consisted of three steps, which are described in the following.

2.2.1. *Definition of reference periods*

The procedure required expressing the weather data as anomalies relative to a reference climatology. We used different reference climatologies for the historical and present situations. For the former, we used 1800–1820 During this period, no changes occurred to the stations in Geneva and Hohenpeissenberg (Auchmann *et al* 2012). Furthermore, we excluded the volcanically perturbed years 1809–1811 and 1815–1817, as in Auchmann *et al* (2012). Based on data availability (see above), we used 1982–2009 as a reference for the present climate. Thus, the reference periods maximize data availability and minimize inhomogeneity. The reference climate was then obtained from station and gridded data by fitting the first two harmonics of the annual cycle.

To obtain a distance metric, as well as for the weather type classification, the variables (T_{min} and

T_{max}, pressure, pressure tendency and precipitation) were standardized by subtracting their annual cycle and dividing by the standard deviation (s.d.), which was de-seasonalized in the same way. As an exception, temperature in the 1982–2009 period, which exhibits a strong trend, was additionally linearly detrended before standardization.

2.2.2. Analog—level 1: Swiss weather types

Analog days must have similar weather characteristics as the target day. In a first step, we thus restricted our pool of possible analogs to days that share the same general weather type. In order to define one weather type for Switzerland, we first averaged daily pressure, pressure tendency, and wind direction (using a bilinear approach) from the three stations and then standardized the pressure and pressure tendency series. Then, we derived weather types in the same way as in Auchmann *et al* (2012). First, frontal passages were defined as days with very low (<2.5 s.d.) or rapidly rising (>2.5 s.d.) pressure. The remaining days were then partitioned into classes of wind direction (NW or N, NE or E, SE or S, SW or W) and pressure (< −1 s.d., −1 to +0.75 s.d., >0.75 s.d.). The middle pressure class was further subdivided into raising, stationary and falling pressure (using the thresholds ±0.2 s.d.; details are given in Auchmann *et al* 2012). This resulted in a total of 19 weather types. The weather types were defined for both the historical and the present-day periods.

2.2.3. Analog—level 2: distance

For each day in 1816/17, we searched for an analog within the 1982–2009 period. The analog must pertain to the same weather type and must be within a window of ±30 calendar days from the target day. Within these days, we chose the analog that minimized the Euclidian distance of all available meteorological observations (T_{min} and T_{max} for Geneva and Hohenpeissenberg, daily mean temperature for Delémont and precipitation for Geneva). This measure was calculated based entirely on station data. Although precipitation is non-Gaussian, its weight in the distance measure is only 1/6 and (as will be shown later) the analog approach produced very good results.

Once the closest analog day was found, we extracted that day from the gridded data. We used the absolute values of precipitation. For solar radiation and temperature, we multiplied the standardized anomaly with the corresponding standard deviation and added back the climatology. Because of the strong temperature trend within the 1982–2009 period, the average temperature of the climatology was already substantially lower than today. Therefore, we added back only the climatology of the years 2002–2009, which better represented present-day climate. To obtain temperature data for 1816 and 1817, we added a historical reference climatology obtained from the gridded 1982–2009 reference by subtracting the spatially interpolated difference in annual mean temperature between the historical and the 1982–2009 reference period (based on the three stations). For solar radiation and precipitation, no trend was considered (i.e. historical and present scenarios were identical).

2.3. Crop model

Simulation of crop yields was conducted with CropSyst, a multi-year, multi-crop daily time step simulation model for evaluating impacts of climate and crop management at the plot scale (Stöckle *et al* 2003). The model simulates potential biomass growth as a function of intercepted radiation and crop transpiration. Both depend on leaf area development driven by biomass growth and phenology, which is simulated as a temperature-dependent process. We used crop parameter sets for winter barley, potato and grain maize derived by calibration for current Swiss conditions by Klein *et al* (2012).

Soil parameters were specified for clay loam as a representative agricultural soil type on the Swiss Plateau and were derived from the Swiss Soil Monitoring Network. A daily cascade approach was used to simulate soil water infiltration, which considers only downwards water flow. Information on elevation was derived from the Swiss digital elevation model in 25 m resolution provided by the Federal Office of Topography (swisstopo, www.swisstopo.admin.ch). The nitrogen sub-model was disabled to evaluate yield limitations only based on climatic limitations (i.e. sub-optimal temperature, radiation and water availability).

Crop yield was simulated using daily climate information (T_{min}, T_{max}, solar radiation and precipitation) for historical and present reference periods, for the historical years 1816 and 1817, as well as for the corresponding present-day years. Representative sowing dates were selected for the three crops and were kept constant in all simulations: 16 October for winter barley, 23 March for potato and 21 April for grain maize. For realistically modelling historical yields, additional factors such as farming techniques should be considered, but this was beyond the scope of this study.

2.4. Post-processing

Under conditions of high soil moisture, reduced soil aeration limits crop growth and yield. This effect may have played a considerable role in the year 1816, and since CropSyst is not able to capture such effects, an ex-post analysis of simulated soil water saturation was performed. The number of days with 100% soil water saturation and a 'stress day index' (SDI) was calculated, which accounts for differences in crop responses to excess water depending on phenological stage. According to Ravelo *et al* (1982), SDI was calculated as the sum of the product of a susceptibility factor, CS, and a stress day factor, SD, for specific phenological stages. Following Hardjoamidjojo *et al*

Table 2. Differences in seasonal mean temperature and precipitation sum between the years 1816 and 1817 and the historical reference period in observations (Obs) and reconstructions (Rec). Also indicated is the standard deviation (s.d.) and first-order autocorrelation of daily temperature anomalies and precipitation sums as well as the correlation between Obs and Rec. Pearson correlations are used for temperature, Spearman correlations for precipitation.

	Temperature (°C)		Precipitation (mm)	
Season	Obs	Rec	Obs	Rec
JFM 1816	−0.30	−0.53	−9	−32
AMJ 1816	−1.34	−2.28	71	89
JAS 1816	−2.27	−1.98	109	96
OND 1816	−0.04	−0.69	−19	−62
JFM 1817	2.30	1.12	10	−15
AMJ 1817	−1.10	−2.22	8	−31
JAS 1817	0.26	0.46	33	−21
OND 1817	−0.51	−1.41	−83	−137
s.d.	3.39	3.28	5.87	5.49
ρ_1	0.76	0.68	0.21	0.30
r(Obs)		0.86		0.67

(1982), SD was defined as the sum of soil water content (in mm) above the 30 cm level. Values for CS were used according to Evans and Skaggs (1984): 0.16 (crop establishment), 0.18 (early vegetative stage), 0.38 (late vegetative stage), 0.21 (flowering), 0.06 (yield formation).

3. Results

3.1. Weather data

The weather reconstruction was assessed with respect to bias, autocorrelation, variability, and extremes. A comparison of the gridded reconstructions for 1816 and 1817 with the original observations for Geneva (table 2) shows that seasonal mean anomalies are well reproduced in the reconstruction approach. Overall, reconstructions are somewhat too cold, most pronounced in spring of 1816. The same is found in the series of Delémont (not shown).

The time series for observed and reconstructed daily mean temperatures and precipitation sums in Geneva are shown in figure 2 for the year 1816. Correlations (table 2) are 0.86 for temperature anomalies and 0.67 for precipitation, respectively. The agreement is excellent with respect to both the magnitude of the anomalies and the sequence and length of the cold spells or wet spells. The variance of the anomalies as well as the first-order autocorrelation (table 2) also agree well between reconstructions and observations.

Data from Geneva and Delémont entered the reconstruction, so they are not independent. The daily fields were also evaluated by comparing the reconstructed data with an independent series from Aarau, for the year 1816 (for this comparison, all series were deseasonalized by subtracting the first two harmonics of the year 1816). Correlations for temperature are 0.68, 0.66, and 0.73 for T_{min}, T_{max} and mean temperature. The lower correlation compared with those with Geneva and Delémont can be explained by the lower reporting precision of the Aarau data (1° Réaumur, i.e. 1.25 °C), and the fact that the Aarau data are in raw format and thus potentially affected by error. Nevertheless, the agreement shows that the reconstructions capture the most important features of variability. Furthermore, the reconstruction approach guarantees that precipitation and temperature fields of each day are mutually consistent.

Finally, the spatial patterns of the anomalies are consistent with the expected climatic processes. Figure 3 shows anomaly fields (relative to 1800–1820) of T_{min}, T_{max}, precipitation, and radiation averaged over the growing season. T_{max} is reduced in most areas (more strongly north of the Alps), while T_{min} is reduced less strongly in those areas that are normally affected by cold air drainage flows. This is consistent with an analysis of station data in Brönnimann and Krämer (2016) and is expected from the work of Auchmann *et al* (2012, 2013) who found that cloud cover was one of the main influences on temperature anomalies at that time.

The precipitation anomaly shows the imprint of weather systems travelling across Switzerland from the west or northwest and of orographically enhanced rainfall along the northern slope of the Alps. This is also mirrored in the radiation reconstruction. Overall, we conclude that the reconstruction is physically consistent, statistically appropriate and spatially meaningful (showing changes in cold air drainage).

3.2. Crop phenology

Table 3 presents simulated shifts in phenological phases for winter barley, potato and maize. Since the crop model could only be calibrated for current crops and cultivars in Klein *et al* (2012), the simulated changes cannot be considered fully representative for crops and cultivars grown in the 19th century. Emergence is clearly delayed in all modelled crops in the first year after the eruption (yr 1) and is even more delayed in the following year (yr 2) because of an exceptionally cold spring in 1817. Except for winter barley, the delay of the remaining phenological phases is smaller in yr 2 as compared to yr 1. For yr 1, the longest delay is found for maize (4–7 weeks), except for harvest date, which for this crop is fixed in the simulations. The longest delay in harvest date of 3 weeks is obtained for potato.

It is important to note that modelled delays in phenological phases and their differences between seasons and years are largely consistent with patterns in observed shifts (tables 3 and 4). Phenological dates are available from observations reported in historical documents for the Swiss Plateau (from EURO-CLIMHIST, Pfister 2015, http://www.euroclimhist.unibe.ch/en), though not for the same crops and the

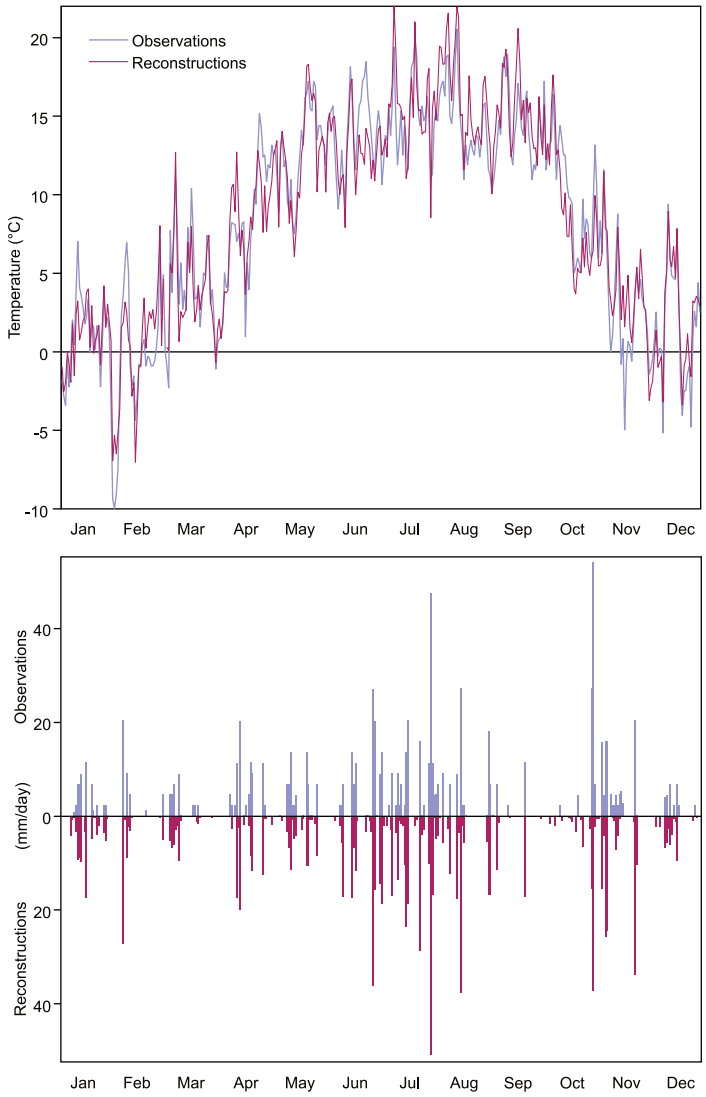

Figure 2. Time series of daily mean temperature (top) and precipitation (bottom) for 1816 from observations and the reconstruction.

same phenophases. Long time series are available for grapevine, rye and cherry on the Swiss Plateau. Table 4 shows shifts in the dates of phenological stages in 1816 and 1817 relative to the average for the same reference period (1800–1820 without volcanically perturbed years). An average delay of 2–4 weeks is found for all summer and autumn phenophases in 1816. Spring phases are delayed less, similar as for maize in the model simulation. It should be noted that the dates for grape harvest in 1816 could not be seen as 'true' phenological dates as grapes did not ripe at all and were harvested unripe.

Differences between observed and simulated phenological shifts in 1817 may be attributed to differences in thermal requirements and seasonality of observed and simulated crops, remaining biases in the reconstructions (see table 2) and differences in climatic reference periods.

3.3. Potential yields

Modelled crop yields for the historical 1816 scenario show a substantial reduction (figure 4). For potato, the decrease relative to the historical reference period amounts to 20%–40%. Even higher losses are found in marginal areas near the production limit such as at higher altitudes. This is roughly the order of magnitude of reductions observed in 1816 for many crops. Smaller reductions are found for winter barley. Lower yields are also modelled for 1817 (not shown).

Relative crop losses for the present-day scenario are almost identical to those from the historical simulations. We find strong losses in potato and even stronger losses in maize, but smaller losses for winter barley. The second year (corresponding to 1817) still shows a substantial reduction, which is largely due to the cold spells in spring.

The observed increase in grain prices between January 1816 and early summer 1817 exhibited a clear east-west gradient (figure 4, top right). Yield simulations for potato reveal only a small gradient with large losses in both eastern and western regions, while for maize, simulations reveal a strong east-west gradient (figure 5, for the situation today). This gradient is related to the effect of increasing altitude

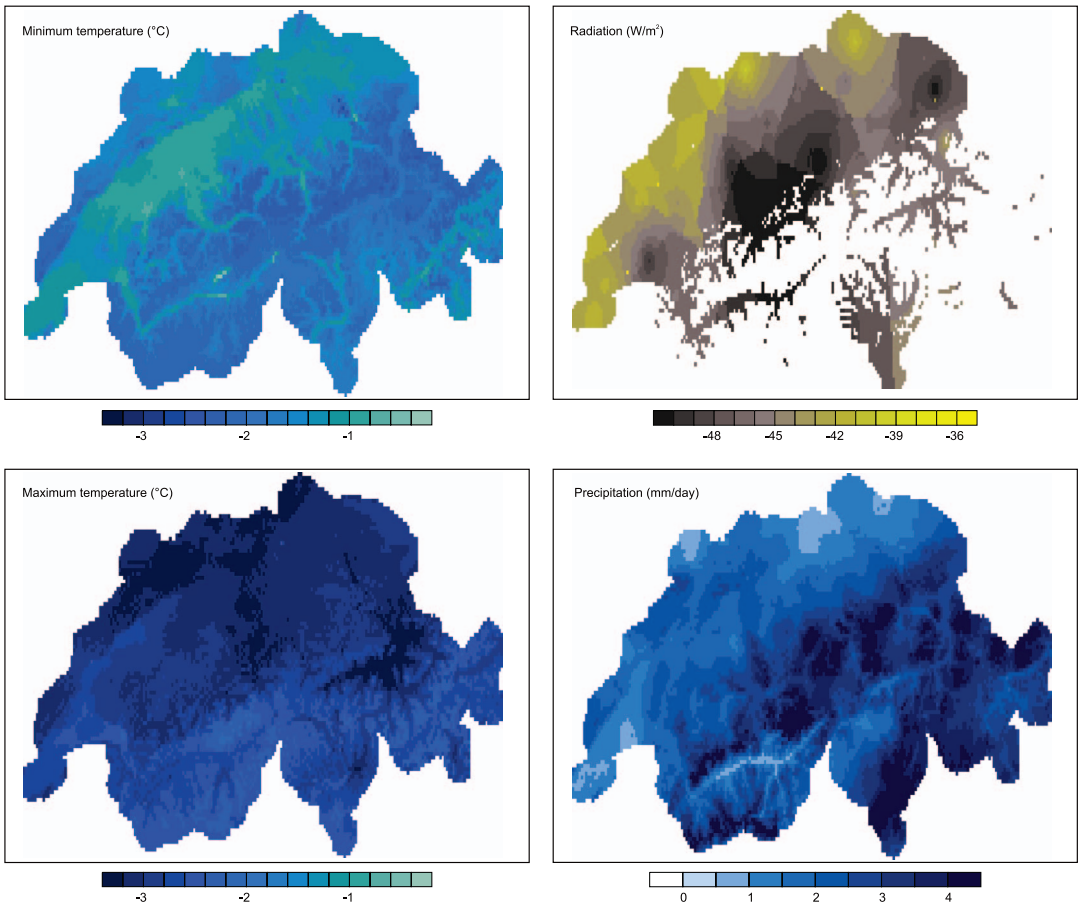

Figure 3. Reconstructed anomaly fields over the growing season (April to September) 1816 with respect to the historical reference period for T_{min} and T_{max}, solar radiation, and precipitation. Weather data are only used below 1500 m asl. For radiation, which in contrast to the other fields was interpolated from stations, we did not derive values above 1500 m asl.

Table 3. Modelled days of phenological phases for the present period (ref, in day-of-year) as well as deviations from the reference for the first and second year after the eruption (deviation in number of days).

	Barley			Potato			Maize		
Phenological stage	Ref	yr 1	yr 2	Ref	yr 1	yr 2	Ref	yr 1	yr 2
Emergence	301	+5	+11	110	+10	+15	128	+5	+10
Flowering	164	+3	+6	162	+13	+12	173	+48	+41
Grain/tuber filling	175	+5	+7	207	+19	+13	228	+28	+13
Harvest	213	+6	+8	219	+21	+13	275	0	0

Table 4. Phenological data from observations for the historical reference period (Ref, in day-of-year) as well as deviations in 1816 and 1817 (deviation in number of days). Data from Pfister (2015).

Location	Plant	Phenological stage	Ref	1816	1817
Zollikon	Grape	Bud burst	114	+3	+16
Swiss Plateau	Cherry	Flowering	114	+4	+16
Zollikon	Grape	Flowering	158	+31	+20
Zollikon	Grape	First fruit	188	+26	+14
Swiss Plateau	Rye	Harvest start	205	+17	+5
Zollikon	Grape	Coloring	234	+25	+15
Swiss Plateau	Grape	Harvest start	290	+20	+7
Zollikon	Grape	Harvest start	292	+11	+4

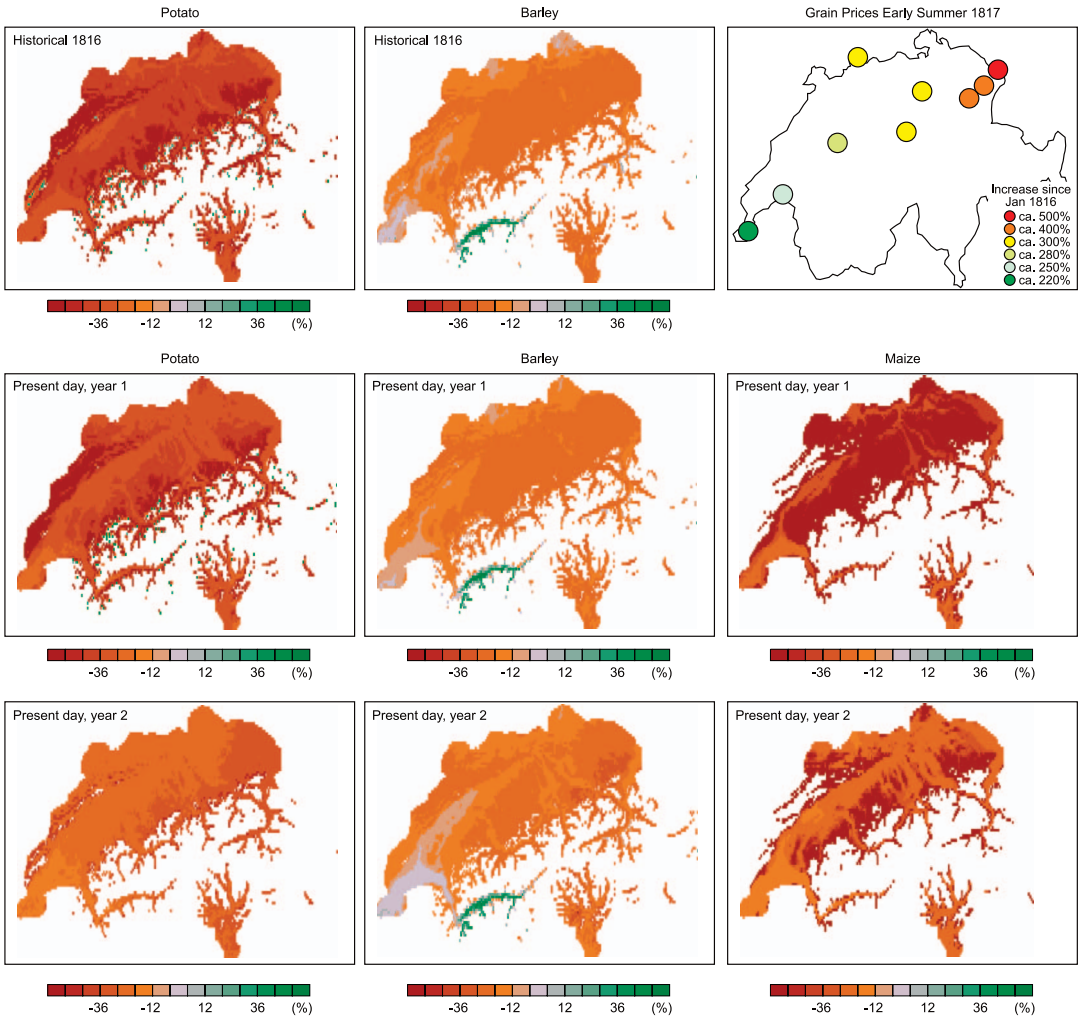

Figure 4. Reduction of harvested crop yields for the first post-eruption year in the historical period (top) and as well as the first and second post-eruption year in the present period (middle and lower column) relative to the corresponding references. The top right panel shows the increase in the prices of the major grains in several Swiss markets from January 1916 to early summer 1817 (from Krämer 2015).

towards eastern Switzerland, and to a declining gradient in radiation. For barley, a weaker gradient exists compared to maize (not shown).

The stress factor approach allows assessing consequences of waterlogging in qualitative terms (figure 5). In the 1816 scenario, the number of days with 100% soil saturation is much higher than in the reference (middle panel) or in the 1817 scenario. Again, an east-west gradient appears with soil saturation increasing towards the eastern regions. The 'stress day index' (bottom panel) accounts not only for days with 100% saturated soils but also other days with a high soil water level. As a consequence, the 1817 scenario, which was clearly less rainy than in 1816, also exhibits a high stress index. Assuming yield losses to be proportional to the stress index, additional substantial crop losses due to the effect of waterlogging are likely in both years, with higher losses in the eastern compared to the western part of the Swiss Plateau. Note that precipitation and radiation are the same in the 1816/1817 and the corresponding present-day scenarios. Thus, the stress index is also very similar.

4. Discussion and conclusions

Despite limitations of the crop model simulations, such as lack of effects due to pests and pathogens, our approach provides, for the first time, a quantitative picture of crop yield losses following the YWAS of 1816, starting from weather reconstructions and using a process-based crop model. The weather reconstruction realistically depicts the daily weather of 1816 and 1817 and thus is a useful scenario to study possible effects of such a massive volcanic eruption on agricultural crop production under today's conditions.

Modelled crop yields for the years 1816/17 following the Tambora eruption, as well as for a similar scenario today, show substantial losses in the range of several tens of percent for currently cultivated important crops. The delay in phenologial phases and yield losses agree well with documentary observations both in 1816 and 1817. While crop development rate is mainly driven by temperature, potential yields are strongly influenced by intercepted radiation until harvest. In 1816, low temperatures and low solar irradiance decreased growth and yields, while negative

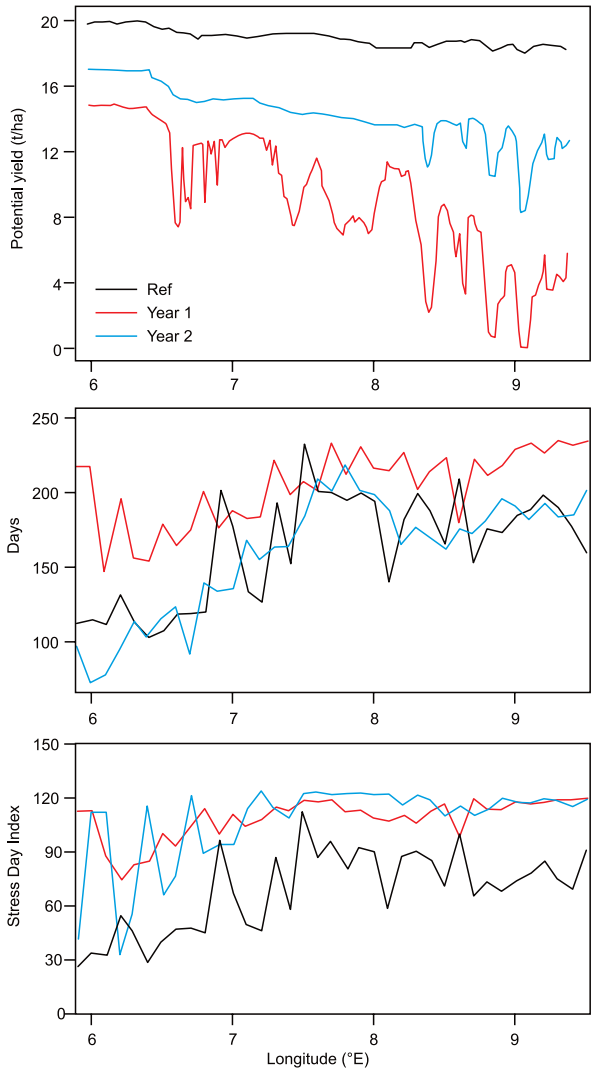

Figure 5. West-East transects (see figure 1) referring to the reference period today, year 1 and year 2 of (top) potential maize yields, (middle) the number of days with 100% soil saturation and (bottom) the stress day index. Note that the latter two were not calculated for every grid point and thus the spatial resolution is lower.

effects in 1817 were mainly due to cold conditions in spring (note that temperatures in 1817 are underestimated in the reconstructions, arguably contributing to an overestimation of the delay of phenophases in 1817 in the model). In addition to low temperature and reduced radiation, a large amount of precipitation leading to waterlogging negatively affected yields both in 1816 and in 1817.

For the situation of a Tambora-type eruption occurring in the present climate, followed by a YWAS, our model simulations suggest decreases in yields of today's crops of almost the same magnitude as in 1816. Losses are highest for current maize hybrids (not cultivated in 1816) and amount to 30%–50% (note that to these losses, the effects of waterlogging need to be added). It should be considered that in the simulations land use and land use decisions were not incorporated, and only the climate-limited crop yield could be estimated with the model. Moreover, in 1816/1817 losses along the value chain were very large and, hence, in a full assessment of food shortage effects of trade, market regulations, and other factors should be addressed. Finally, our assessment does not consider crop quality, which was reportedly low in 1816 (Krämer 2015). Since the crop model is not able to capture impacts of waterlogging, pests and diseases, it cannot be precluded that any of these factors may have added to the east-west divide in malnutrition. Especially fungal diseases and waterlogging may have had detrimental effects on crop yields and quality.

The simulations reveal an east-west gradient in yield loss across the Swiss Plateau despite the fact that neither precipitation nor temperature shows a clear gradient. This is found most strongly for maize for which it could be attributed to differences in altitude and radiation. However, maize was not cultivated and the gradient is small for potato, relative to the recorded historical difference in price (figure 4). Although there are remaining uncertainties, it is unlikely that spatial differences in yield losses are solely responsible for the observed differences in malnutrition. It is more likely, and in agreement with the work by historians (Krämer 2015), that they were caused mainly by economic, political and social factors.

In contrast to the situation in 1816/17, and assuming no large-scale market effects of crop losses, short-term reductions in food supply due to a loss in domestic crop yields in the order of 30%–40% would seem manageable within the current technical, economic and political situation in Switzerland, given current emergency plans, information systems including accurate medium-range weather forecasts, and the lead time between a volcanic eruption and effects. However, an eruption climate scenario might have a disruptive effect on the global food system (Puma *et al* 2015), which indirectly could affect food availability and prices in Switzerland.

An important lesson learned from studying the Tambora eruption and subsequent YWAS is that a mono-causal argumentation leading from the volcanic eruption to societal impacts is not an appropriate way to think about climate-society interactions (Brönnimann and Krämer 2016). While such a link can indeed be made, and our model simulations presented here are a part of such a deterministic chain, we find that at each step, other influences matter, and perhaps even dominated the response. For instance, the Tambora eruption explains only one (arguably minor) part of the YWAS. Furthermore, adverse weather is not the only factor affecting crop yields, and yields do not directly translate into prices and societal impacts. The crises of 1817 following the YWAS hit in the worst possible moment a society that was vulnerable, in a phase of political transition, with poor governance, a down turning economy, and lack of reserves (Brönnimann and Krämer 2016). Yet, also in the future, there will be countries and societies vulnerable to a severe climatic event. Modelling tools to quantitatively investigate possible climatic effects on such subsystems can strengthen a society's adaptive capacity by providing relevant information for adaptation planning. However, socio-economic factors play a very important role in determining how successfully a society will be able to respond to extreme climate events. Therefore, interdisciplinary efforts in research and implementation are necessary for designing proactive strategies to improve the resilience of the respective food systems.

Acknowledgments

This work was supported by the Swiss National Science Foundation (projects CHIMES and EXTRA-LARGE). We acknowledge the support by Martin Grosjean and the Oeschger Centre for Climate Change Research of the University of Bern and the PAGES working group VICS (Volcanic Impacts on Climate and Society).

References

Auchmann R, Brönnimann S, Breda L, Bühler M, Spadin R and Stickler A 2012 Extreme climate, not extreme weather: the summer of 1816 in Geneva, Switzerland *Clim. Past Discuss.* **7** 3745–74

Auchmann R *et al* 2013 Impact of volcanic stratospheric aerosols on diurnal temperature range (DTR) over the past 200 years: Observations versus model simulations *J. Geophys. Res.* **118** 9064–77

Bider M, Schüepp M and von Rudloff H 1959 Die Reduktion der 200 jährigen Basler Temperaturreihe *Arch. Met. Bioklim.* **B9** 360–411

Brázdil R, Reznícková L, Valášek H, Dolák L and Kotyza O 2016 Climatic effects and impacts of the 1815 eruption of Mount Tambora in the Czech Lands *Clim. Past* **12** 1361–74

Brönnimann S and Krämer D 2016 Tambora and the 'year without a summer' of 1816. A perspective on earth and human systems science *Geographica Bernensia* **G90** p 48

Brugnara Y *et al* 2015 A collection of sub-daily pressure and temperature observations for the early instrumental period with a focus on the 'year without a summer' 1816 *Clim. Past* **11** 1027–47

Evans R O and Skaggs R W 1984 Crop susceptibility factors for corn and soybeans to controlled flooding *ASAE Paper* 84–2567 (ASAE, St Joseph)

Frei C 2013 Interpolation of temperature in a mountainous region using nonlinear profiles and non-euclidean distances *Int. J. Climatol.* **34** 1585–605

Hardjoamidjojo S, Skaggs R W and Schwab G O 1982 Corn yield response to excessive soil water conditions *Trans. ASAE* **25** 922–7

Klein T, Calanca P, Holzkämper A, Lehmann N, Roesch A and Fuhrer J 2012 Using farm accountancy data to calibrate a crop model for climate impact studies *Agr. Syst.* **111** 23–33

Krämer D 2015 «*Menschen grasten nun mit dem Vieh*» Die letzte grosse Hungerkrise der Schweiz 1816/17 (Basel: Schwabe) p 527

Luterbacher J and Pfister C 2015 The year without a summer *Nat. Geosci.* **8** 246–8

MeteoSwiss 2013a Documentation of Meteoswiss grid data products: Daily mean, minimum and maximum temperature: TabsD, TminD, TmaxD *Federal Office of Meteorology and Climatology MeteoSwiss* 4 pp

MeteoSwiss 2013b Documentation of Meteoswiss grid data products: Daily precipitation (final analysis): RhiresD *Federal Office of Meteorology and Climatology MeteoSwiss* p 4

Oppenheimer C 2003 Climatic, environmental and human consequences of the largest known historic eruption: Tambora volcano (Indonesia) 1815 *Prog. Phys. Geogr.* **27** 230–59

Pfister C 2015 *Module Switzerland* ed C Pfister and C Rohr Data-base Euro-Climhist (http/www.euroclimhist.unibe.ch/en/) (Accessed: 3 November 2016)

Post J D 1977 *The Last Great Subsistence crisis in the Western World* (Baltimore: Johns Hopkins University Press) p 240

Puma M J, Bose S, Chon S Y and Cook B I 2015 Assessing the evolving fragility of the global food system *Environ. Res. Lett.* **10** 024007

Ravelo C J, Reddell D L, Hiler E A and Skaggs R W 1982 Incorporation of crop needs into drainage system design *Trans. ASAE* **25** 623–9

Raible C C *et al* 2016 Tambora 1815 as a test case for high impact volcanic eruptions: Earth system effects *WIREs Clim. Change* **7** 569–89

Schüepp M 1961 *Lufttemperatur* Beiheft zu den Annalen der SMZ, Zürich

Stöckle C O, Donatelli M and Nelson R 2003 CropSyst, a cropping systems simulation model European *J. Agronomy* **18** 289–307

Veale L and Endfield G H 2016 Situating 1816, the 'year without summer', in the UK *Geogr. J* **182** 318–30

Winkler P 2009 Revision and necessary correction of the long-term temperature series of Hohenpeissenberg, 1781–2006 *Theor. Appl. Climatol.* **98** 259–68